Journal of Hydrology 559 (2018) 721–735

Contents lists available at ScienceDirect

Journal of Hydrology

journal homepage: www.elsevier.com/locate/jhydrol

Research papers

An efficient soil water balance model based on hybrid numerical and statistical methods

Wei Mao [a], Jinzhong Yang [a], Yan Zhu [a,*], Ming Ye [b], Zhao Liu [c], Jingwei Wu [a]

[a] State Key Laboratory of Water Resources and Hydropower Engineering Science, Wuhan University, Wuhan, Hubei 430072, China
[b] Department of Earth, Ocean, and Atmospheric Science, Florida State University, Tallahassee, FL 32306, USA
[c] Jiangxi Institute of Soil and Water Conservation, Nanchang, Jiangxi 330029, China

ARTICLE INFO

Article history:
Received 28 January 2018
Received in revised form 25 February 2018
Accepted 26 February 2018
Available online 27 February 2018
This manuscript was handled by Corrado Corradini, Editor-in-Chief

Keywords:
Water balance model
Drainage function
Upward flow
Heterogeneity
Regression method
Coarse discretization in space and time

ABSTRACT

Most soil water balance models only consider downward soil water movement driven by gravitational potential, and thus cannot simulate upward soil water movement driven by evapotranspiration especially in agricultural areas. In addition, the models cannot be used for simulating soil water movement in heterogeneous soils, and usually require many empirical parameters. To resolve these problems, this study derives a new one-dimensional water balance model for simulating both downward and upward soil water movement in heterogeneous unsaturated zones. The new model is based on a hybrid of numerical and statistical methods, and only requires four physical parameters. The model uses three governing equations to consider three terms that impact soil water movement, including the advective term driven by gravitational potential, the source/sink term driven by external forces (e.g., evapotranspiration), and the diffusive term driven by matric potential. The three governing equations are solved separately by using the hybrid numerical and statistical methods (e.g., linear regression method) that consider soil heterogeneity. The four soil hydraulic parameters required by the new models are as follows: saturated hydraulic conductivity, saturated water content, field capacity, and residual water content. The strength and weakness of the new model are evaluated by using two published studies, three hypothetical examples and a real-world application. The evaluation is performed by comparing the simulation results of the new model with corresponding results presented in the published studies, obtained using HYDRUS-1D and observation data. The evaluation indicates that the new model is accurate and efficient for simulating upward soil water flow in heterogeneous soils with complex boundary conditions. The new model is used for evaluating different drainage functions, and the square drainage function and the power drainage function are recommended. Computational efficiency of the new model makes it particularly suitable for large-scale simulation of soil water movement, because the new model can be used with coarse discretization in space and time.

1. Introduction

Since 1970s, various numerical methods have been developed to simulate saturated-unsaturated soil water movement at various temporal and spatial scales (Bastiaanssen et al., 2007; Ranatunga et al., 2008; Pan et al., 2015; Vereecken et al., 2016; Yang et al., 2016). Among them, the two major approaches are numerical solutions of the Richards' equation and the reservoir cascade scheme (Richardson, 1922; Gandolfi et al., 2006; Wesseling, 2009). Based on the principle of mass conservation and the Darcy-Buckingham law, the Richards' equation is the fundamental governing equation that describes unsaturated flows, and its numerical solutions have been implemented in many public-domain and commercial software, such as HYDRUS (Šimunek et al., 2008), SWIM (Huth et al., 2012), FEFLOW (Diersch, 2013), MIKE-SHE (Graham and Butts, 2005), and TOUGH (Xu et al., 2012; Gu and Riley, 2010). The Richards' equation has solid theoretical foundation, and its numerical solutions have been widely used in studies of groundwater resources assessment, groundwater pollution, land subsidence, sea water invasion, soil water and salt transport, and agricultural water management (Yang et al., 2016). However, using Richards' equation requires intensive input data and model parameters, which are not always available in practice. In addition, the computational cost for large-scale modeling is high due to the highly nonlinearity of the Richards' equation (Hayek, 2016; Liu et al., 2016; Downer and Ogden, 2004; Shen and Phanikumar, 2010).

* Corresponding author.
E-mail address: zyan0701@163.com (Y. Zhu).

https://doi.org/10.1016/j.jhydrol.2018.02.074
0022-1694/

The problems above associated with the Richards' equation can be resolved or alleviated by using the reservoir cascade scheme employed to solve water balance models (also known as conceptual models) that are physically based on water mass balance. In the water balance models, simplified or empirical equations (different from the Darcy-Buckingham law) are used to describe soil water movement (Zha, 2014). Many water balance models are currently in use because of their computational efficiency and stability, especially in large-scale modeling where data and fundamental understanding of the factors and processes of soil water movement are lacking (Ranatunga et al., 2008). The widely used water balance models include SWAT (Arnold et al., 2012; Abeysingha et al., 2015), INFIL 3.0 (FILL, 2008), SoilWat (Holzworth et al., 2014), DSSAT (Jones et al., 2003), BUDGET (Raes, 2002), Hydrobal (Bellot and Chirino, 2013), and SWB (Westenbroek et al., 2010).

The major hydrological processes considered in water balance models include precipitation, runoff, plant interception, evaporation, transpiration, infiltration, redistribution, and drainage or deep percolation (Ranatunga et al., 2008). The water balance models generally handle the major hydrological processes separately and use physically meaningful parameters to describe individual processes. The major soil hydrological processes are driven by the water potential, which is composed of the matric potential and the gravitational potential in unsaturated zone (Yang et al., 2016). Many water balance models assume that the gravitational potential dominates over matric potential, and therefore neglect matric potential and only simulate downward soil water flow driven by gravitational potential (Arnold et al., 2012; FILL, 2008; Jiang et al., 2008). As a result, the "tipping-bucket" method (Kendy et al., 2003; Riha et al., 1994) has been used to describe the infiltration, redistribution, and drainage processes. In the vertical direction, a soil column is divided into a cascade of "buckets"; each "bucket" corresponds to a soil layer and can be filled by infiltration and emptied by evapotranspiration and/or drainage. Specifically speaking, the infiltration water first fills the top "bucket", then the excessive infiltration water moves downward to the next "bucket", until all the infiltration water is allocated in the buckets. Subsequently, the soil water redistribution happens, driven by the gravity. The soil water can percolate into the next bucket when the soil water content exceeds the field capacity of the overlying bucket, and the drainage process is described by a drainage function (Gandolfi et al., 2006). This method is easy to implement numerically without requiring iterative solvers (Riha et al., 1994).

However, the "tipping-bucket" method described above cannot simulate upward soil water movement, because matric potential is neglected and only the gravitational potential is considered (Jiang et al., 2008; Kendy et al., 2003). In other words, due to neglecting matric potential, soil water can only be drained downward by gravitational potential or directly depleted by evapotranspiration. This is a reasonable assumption, when groundwater recharge is the major concern and when the errors introduced by neglecting matric potential is insignificant (FILL, 2008; Kendy et al., 2003; Vaccaro, 2007). However, when the errors alter soil water movement and salt accumulation at top soil due to the upward flow especially in agricultural areas with strong evapotranspiration (Rengasamy, 2006; Valipour, 2014), the assumption of neglecting matric potential becomes invalid.

Another problem of the water balance models is that they generally cannot be used for heterogeneous soils. Take as an example the soil water balance model, SoilWat in APSIM (Holzworth et al., 2014), which originated from CERES-Maize (Adnan et al., 2017). SoilWat considers both upward and downward soil water movement as well as the hydrological processes of runoff, infiltration, evapotranspiration, and redistribution of water by saturated and unsaturated flow. The soil water flow driven by matric potential is calculated by introducing hydraulic diffusivity based on an empirical function. While SoilWat performs well in comparison with SWIMv2 (a numerical model that solves Richards' equation) as shown in Verburg (1995), it cannot be applied to heterogeneous soils, as soil water moisture is not continuous across the boundaries between different soil types (Yang et al., 2009). In addition, to calculate the hydraulic diffusivity, two empirical parameters are required for each soil type, whereas the empirical parameters do not have physical meanings. Furthermore, SoilWat assumes that the evaporation rate is proportional to the square root of time, and the diffusivity soil water movement is calculated in separate loops for upward and downward flow (Verburg, 1995). These are unreasonable simplifications.

In this study, we develop a new one-dimensional water balance model by using hybrid numerical and statistical methods to calculate both upward and downward soil water movement in heterogeneous unsaturated soils. The water flow process within one time-step has the following four components: infiltration allocation, redistribution driven by gravitational potential, source/sink driven by external forces, and diffusion driven by matric potential. These components are evaluated separately by numerically solving their own governing equations. To apply the water balance model to heterogeneous soil, we introduce a correction term to describe spatial variability of soils. The statistical method used in our model simplifies the model parameters, so that the water balance model requires only four parameters that have physical meanings. The parameters are saturated hydraulic conductivity (K_s), saturated water content (θ_s), field capacity (θ_f), and residual water content (θ_r). The details of the water balance model are given in Section 2. In Section 3, two published examples with homogenous and heterogeneous soils are used to test the accuracy of the water balance model, and three synthetic examples are designed to evaluate the model performance for eight soil types. The impacts of five drainage functions and applicability of our model to different discretization resolutions (in space and time) are also evaluated by comparing the modeling results with those obtained by using HYDRUS-1D. Section 3 also includes a real-world application of the model to demonstrate the model's applicability. The conclusions of the merits and demerits of the model are given in Section 4.

2. Model development

Section 2.1 discusses the conceptual model and the governing equations of the water balance model. Three equations are used to describe the driving forces of soil water movement, i.e., the gravitational potential that drives advective soil water movement, external forces acting as source/sink terms (e.g., evapotranspiration), and the matric potential that drives diffusive soil water movement. The three equations are solved sequential, first for the advective movement, then for the source/sink terms, and ultimately for the diffusive movement. Associated with the simulation of the advective soil movement, a brief review for existing formulas used to describe the drainage process is provided. The actual evapotranspiration (a source/sink term) is calculated by using the Penman-Monteith equation (Allen et al., 1998) and the Ritchie-type method (Berengena and Gavilan, 2005; Braud et al., 2005; Raes, 2002). After solving the equation for advective movement and source/sink terms, we solve the diffusion equation to simulate diffusive soil water movement. In this step, hydraulic diffusivity is represented by a new empirical formula that has three parameters (saturated hydraulic conductivity K_s, saturated water content θ_s and residual

Table 1
Empirical drainage functions representing the relationship between the unsaturated hydraulic conductivity $K(\theta)$ and soil water content θ.

Name	Function	Parameters	Application
Linear equation	$K(\theta) = K_s \times \frac{\theta-\theta_f}{\theta_s-\theta_f}$	K_s, θ_s, θ_f	SWAT (Arnold et al., 2012; Dai et al., 2016), SoilWat (Holzworth et al., 2014; Verburg, 1995)
Exponential equation	$K(\theta) = K_s \times \exp\left(-\alpha \times \frac{\theta-\theta_w}{\theta-\theta_w}\right)$	K_s, θ_s, θ_f, θ_w, α	Kendy et al. (2003), Jiang et al. (2008)
Power equation	$K(\theta) = K_s \times \left(\frac{\theta}{\theta_s}\right)^{\beta}$	K_s, θ_s, θ_f, β	SWRRB (Merritt et al., 2003), DPM (Vaccaro, 2007), INFIL 3.0 (FILL, 2008), EPIC (Wang et al., 2012), CREAMS (Adnan et al., 2017)
Exponential approximation equation	$K(\theta) = K_s \times \frac{\exp(\theta-\theta_f)-1}{\exp(\theta_s-\theta_f)-1}$	K_s, θ_s, θ_f,	BUDGET (Raes, 2002), Aquacrop (Abedinpour et al., 2014)
Square equation	$K(\theta) = K_s \times \left[\frac{\theta-\theta_f}{\theta_s-\theta_f}\right]^2$	K_s, θ_s, θ_f,	BOWET (Sluiter, 1998), BEACH (Sheikh et al., 2009)

Note: The parameters K_s, θ_s and θ_f are the saturated hydraulic conductivity (LT^{-1}), the saturated water content (L^3L^{-3}) and the field capacity (L^3L^{-3}); θ_w is the soil water content at wilting point (L^3L^{-3}); α in the exponential equation is a site-specific parameter determined mainly from soil characteristics and it has an inverse relationship with K_s, and the value ranges between 10 and 30 (Jiang et al., 2008); The parameter β in the power equation ensures $K(\theta)$ to approach zero when θ approaches to θ_f, and an empirical formula as $\beta = -2.655/\log(\theta_f/\theta_s)$ is proposed (Gandolfi et al., 2006).

water content θ_r). The heterogeneous situations are also considered. Sections 2.2–2.4 describe the details for solving each equation separately.

2.1. Conceptual model and governing equations

The one-dimensional water balance model for the unsaturated zone has four major components to describe the soil water movement process within one time step, and they are the allocation of the infiltration water, advection driven by the gravitational potential, source/sink term driven by external forces, and diffusion driven by the matric potential. The infiltration water is assumed to be allocated instantaneously after irrigation or precipitation, and the amount of allocated water for a given layer is calculated as

$$q = \min(M \times (\theta_s - \theta), I - I_d), \tag{1}$$

where q is the amount of allocated water per unit area of the layer (L); M is the thickness of the layer (L); θ is the soil water content (L^3L^{-3}) of the layer; θ_s is the saturated water content (L^3L^{-3}) of the layer; I is the quantity of infiltration water per unit area (L); I_d is the allocated amount of infiltration water per unit area specified before the calculation (L). Note that all soil water contents in this paper are in the unit of volumetric soil water content.

The soil water movement of the allocated water is described by the following governing equations:

$$\frac{\partial\theta}{\partial t} = -\frac{\partial K(\theta)}{\partial z}, \tag{2}$$

for advective movement driven by the gravitational potential,

$$\frac{\partial\theta}{\partial t} = -W, \tag{3}$$

for source/sink term, and

$$\frac{\partial\theta}{\partial t} = \frac{\partial}{\partial z}\left(D(\theta)\frac{\partial\theta}{\partial z}\right), \tag{4}$$

for diffusive movement driven by the matric potential, where θ is the soil water content (L^3L^{-3}); t is the time (T); $K(\theta)$ is the unsaturated hydraulic conductivity (LT^{-1}) as a function of soil water content; z is the elevation in the vertical direction (L); W is the source/sink term (T^{-1}) to account for soil evaporation and root uptake term of crop transpiration; $D(\theta)$ is the hydraulic diffusivity (L^2T^{-1}), $D(\theta) = K(\theta) \times \partial h/\partial\theta$, where h is the pressure head (L).

2.2. Advective movement driven by gravitational potential

When the soil water content exceeds the field capacity of a soil layer, the drainage process happens. For each homogeneous layer with the thickness M, by integrating Eq. (2) over M, we have

$$M\frac{d\theta}{dt} = -K(\theta). \tag{5}$$

The unsaturated hydraulic conductivity $K(\theta)$ is a function of soil water content θ. The relationship between $K(\theta)$ and θ can be described by the van Genuchten model that requires five soil hydraulic parameters (van Genuchten, 1980). When the five parameters are not fully known, it is possible to characterize the relation by using empirical formulas with smaller number of soil hydraulic parameters. These empirical formulas are referred to as drainage functions, and the commonly used ones are listed in Table 1.

Eq. (5) is compatible with the drainage functions listed in Table 1. For example, the linear drainage function is chosen for the following mathematical expressions. By substituting $K(\theta) = K_s \times (\theta - \theta_f)/(\theta_s - \theta_f)$ into Eq. (5), after the separation of variables, integrating the equation, and eliminating an integration constant, we obtain the recursion formula of soil water content for a soil layer,

$$\theta^{j+1} = \theta_f + (\theta^j - \theta_f) \times \exp\left(-\frac{K_s}{M \times (\theta_s - \theta_f)} \times \Delta t\right), \tag{6}$$

where j and $j+1$ represent the current and next time steps with an interval of Δt (T). After updating soil water content for the next time step, the corresponding flux out of the layer can be calculated. The out flux is then added to the underlying layer, and the process is repeated for all underlying layers. This computation procedure is applicable to all the drainage functions listed in Table 1, and examples of numerical simulation using different drainage functions are shown in Section 3.

2.3. Source/sink term

Due to the simple form of Eq. (3) used to account for the source/sink term, we can directly integrate the equation over time to obtain

$$\theta^{j+1} = \theta^j - W \times \Delta t. \tag{7}$$

The W term represents actual soil evaporation and crop transpiration, which play an important role in the soil water movement. The Penman-Monteith formula is used in the water balance model, and the process of crop growth is also taken into consideration. The procedure of implementing Eq. (7) is as follows. First, the reference evapotranspiration is calculated using the climate data and the

FAO-Penman-Monteith equation (Allen et al., 1998; Luo et al., 2012; Valipour, 2015). Subsequently, a crop coefficient K_c is used to obtain the crop evapotranspiration ET_c under standard conditions. The Ritchie-type equation (Berengena and Gavilan, 2005; Braud et al., 2005; Raes, 2002) is used to estimate the potential soil evaporation E_p and the potential crop transpiration T_p as follows,

$$E_p = \tau \times ET_c = \exp(-f \times LAI) \times ET_c, \tag{8}$$

$$T_p = ET_c - E_p, \tag{9}$$

where f is a parameter accounting for the interception of incoming solar radiation by the vegetation (–); LAI is the leaf area index (–).

The E_p and T_p are assigned to soil layers by the evaporation cumulative distribution function and the root density function, respectively. The two functions are decrement functions of soil depth and can ensure the major proportion of soil evaporation and crop transpiration occurring in the topsoil. The actual soil evaporation and crop transpiration are obtained by discounting E_p and T_p with the soil water stress coefficient, and the method for calculating the two coefficients are derived from FAO-56 (Allen et al., 1998).

The actual crop transpiration is calculated as follows,

$$T_a = K_T \times T_p, \tag{10}$$

$$K_T = \max\left[0, \min\left(1, \frac{\theta - \theta_w}{\theta_c - \theta_w}\right)\right], \tag{11}$$

$$\theta_c = \theta_w + (1 - P_W) \times (\theta_f - \theta_w), \tag{12}$$

$$P_W = P_{tab} + 0.04 \times (5 - ET_c), \tag{13}$$

where K_T is the soil stress coefficient for transpiration (–); P_W is the mean fraction of the total available water that can be depleted from the root zone before soil water content stress occurs (–); P_{tab} is a parameter related to the crop type (–) (Allen et al., 1998). The actual soil evaporation is calculated via

$$E_a = K_e \times E_p, \tag{14}$$

$$K_e = \frac{\theta - \theta_d}{\theta_f - \theta_d}, \tag{15}$$

where K_e is the soil stress coefficient for soil evaporation (–); θ_d is the minimum water content under the air dying condition (L^3L^{-3}), and which is set as the residual water content (θ_r). Lastly, the Eq. (7) will be solved by substituting the actual soil evaporation and crop transpiration for each layer.

2.4. Diffusive soil movement driven by matric potential

2.4.1. Diffusion equation

The diffusion equation (Eq. (4)) is discretized using an implicit finite difference method, and then solved with the chasing method of Householder (2006). The discrete equation in layer i (shown in Fig. 1) in a homogeneous soil column is,

$$M_i \frac{\theta_i^{j+1} - \theta_i^j}{\Delta t} = -D_{i-1/2}^j \frac{\theta_i^{j+1} - \theta_{i-1}^{j+1}}{\frac{M_{i-1}}{2} + \frac{M_i}{2}} + D_{i+1/2}^j \frac{\theta_{i+1}^{j+1} - \theta_i^{j+1}}{\frac{M_{i+1}}{2} + \frac{M_i}{2}}, \tag{16}$$

where subscript i represents the layer number and the superscript j represents the time level; M_{i-1}, M_i and M_{i+1} represent the thickness (L) of the soil layers denoted by indices $i-1$, i and $i+1$, respectively; $D_{i-1/2}^j$ represents the geometric mean hydraulic diffusivity (L^2T^{-1}) of layer $i-1$ and layer i at the time level j, and $D_{i+1/2}^j$ represents the geometric mean hydraulic diffusivity (L^2T^{-1}) of layer i and layer $i+1$ at the time level j; θ_i^j, θ_i^{j+1} represent the soil water content ($L^3\,L^{-3}$) of layer i at the time levels j and $j+1$; θ_{i+1}^{j+1}, θ_{i-1}^{j+1} represent the soil water content ($L^3\,L^{-3}$) of layer $i+1$ and layer $i-1$ at the time level $j+1$; Δt is the time step (T).

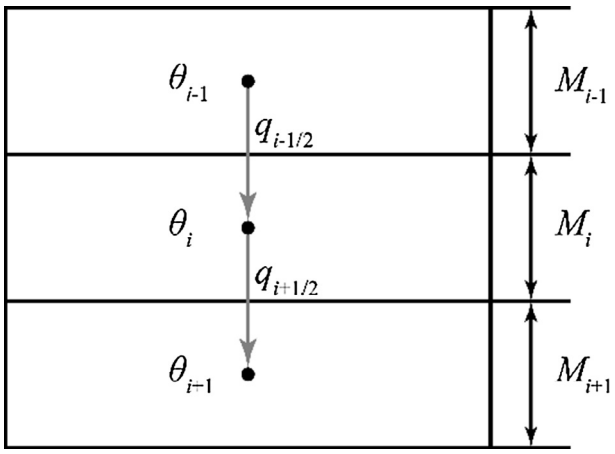

Fig. 1. Sketch for the discrete equation of layer i.

2.4.2. Simplified expression of hydraulic diffusivity

The hydraulic diffusivity of the unsaturated soil is a non-linear function that depends on the soil water content, soil texture, and structure. When using the van Genuchten model (van Genuchten, 1980) to represent the soil water characteristics, the hydraulic diffusivity function is

$$D(\theta) = \frac{K(\theta)}{-m \times n \times \alpha^n \times (\theta_s - \theta_r) \times \{1 + [\alpha \times |h|]^n\}^{-m-1} \times h^{n-1}}, \tag{17}$$

$$K(\theta) = K_s \times \sqrt{S} \times \left\{1 - \left[1 - S^{\frac{1}{m}}\right]^m\right\}^2, \tag{18}$$

$$S = \frac{\theta - \theta_r}{\theta_s - \theta_r}, \tag{19}$$

where h is the pressure head (L); θ is the soil water content ($L^3\,L^{-3}$); θ_s and θ_r are the saturated and residual water content, respectively ($L^3\,L^{-3}$); $K(\theta)$ is the unsaturated hydraulic conductivity (LT^{-1}); K_s is the saturated hydraulic conductivity (LT^{-1}); S is the effective saturation (–); α (L^{-1}) and n are the two empirical parameters; $m = 1 - 1/n$. Five parameters are needed to evaluate Eq. (17), and they are θ_s, θ_r, K_s, α and n.

Since parameters α and n are always difficult to obtain (Zhu et al., 2009; Sun et al., 2015; Vereecken et al., 2010), we develop an empirical formula of hydraulic diffusivity to reduce the number of needed parameters from 5 to 3 (i.e., K_s, θ_s and θ_r); parameters α and n are not needed in the empirical formula. Since the empirical formula has an exponential form and is a straight line in the semi-logarithmic coordinate system, we can fit the hydraulic diffusivity of different soils by the linear regression method as shown in Fig. 2, and the exponential function is

$$D(\theta) = 10^{a \times S(\theta) + b}, \tag{20}$$

where a and b are the slope and intercept of a fitted straight line; S is the effective saturation (–). The soil hydraulic parameters for each soil type refer to Carsel and Parrish (1988) and Carsel et al. (1988), which depend on a soil database including approximately 3000 soils obtained from the U.S. Soil Conservation Service. The regression is mainly based on the soil water content ranging from the field capacity to the saturated water content. The fitted line is extrapo-

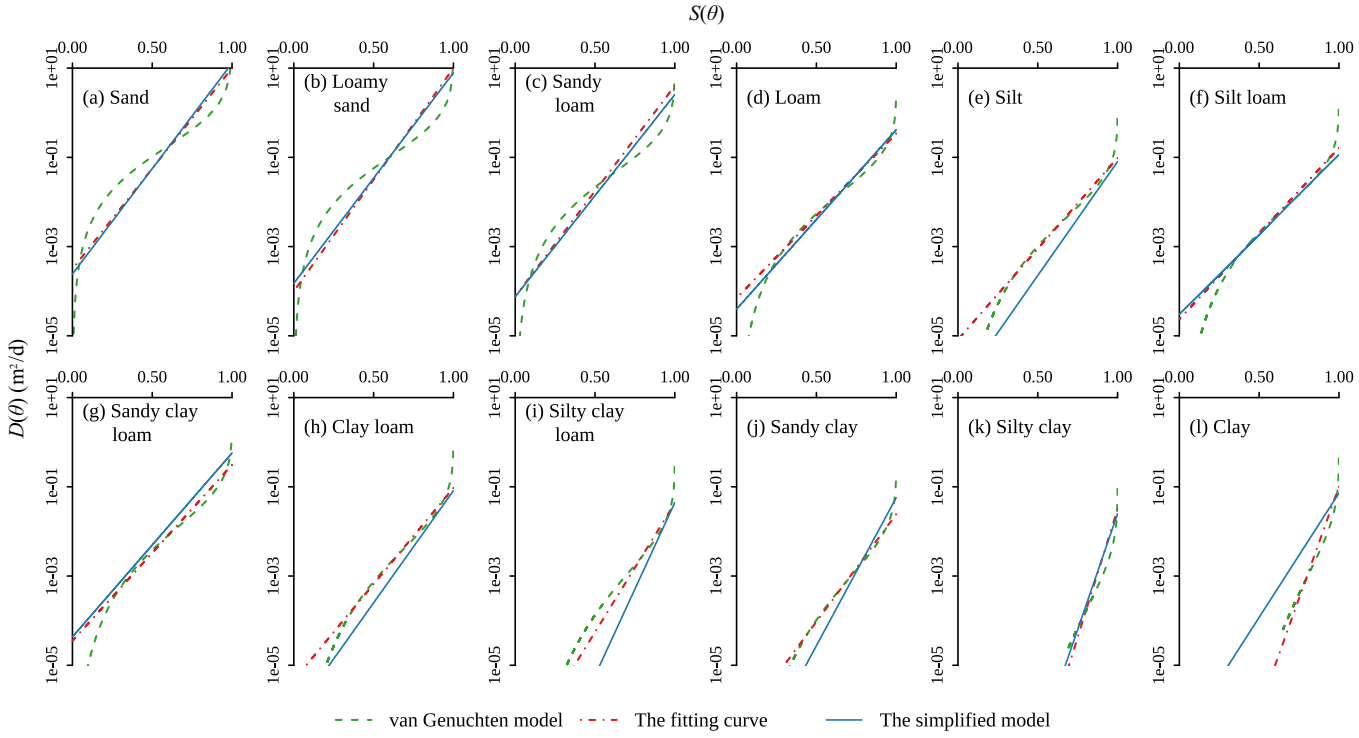

Fig. 2. The comparison of the hydraulic diffusivity curves of the van Genuchten model (green line), the fitting curves by the straight lines (red line) and the simplified model calculated by Eqs. (20)(22) (blue line). (For interpretation of the references to colour in this figure legend, the reader is referred to the web version of this article.)

lated to the soil water content that is smaller than the field capacity. The fitted hydraulic diffusivity by the simplified model is usually larger than the values calculated by using the van Genuchten model when the soil is dry, as shown in Fig. 2. However, the hydraulic diffusivity values are between 10^{-8} m^2/d and 10^{-4} m^2/d for different soil types when the soil water content is close to field capacity. These small values of hydraulic diffusivity will result in limited the soil water movement. The values are even smaller when the soil water content is below the field capacity, for which situation the simplified model cannot result in significant deviations.

We next establish the relationship between the two coefficients (a and b) and the saturated hydraulic conductivity by using the piecewise fitting method with the combination of a quadratic curve and a straight line, as shown in Fig. 3. The resulting regression equations are

$$a=\begin{cases}-0.4014\times\log_{10}(K_s)^2+0.5861\times\log_{10}(K_s)+4.518 & \log_{10}(K_s)\geqslant -0.9\\ -4.8045\times\log_{10}(K_s)-0.7639 & \log_{10}(K_s)<-0.9\end{cases}, \tag{21}$$

$$b=\begin{cases}0.12\times\log_{10}(K_s)^2+0.511\times\log_{10}(K_s)-4.1381 & \log_{10}(K_s)\geqslant -0.9\\ 5.2687\times\log_{10}(K_s)+0.2358 & \log_{10}(K_s)<-0.9\end{cases}. \tag{22}$$

By following the two steps above, the hydraulic diffusivity of a specific soil type can be formulated by the exponential empirical

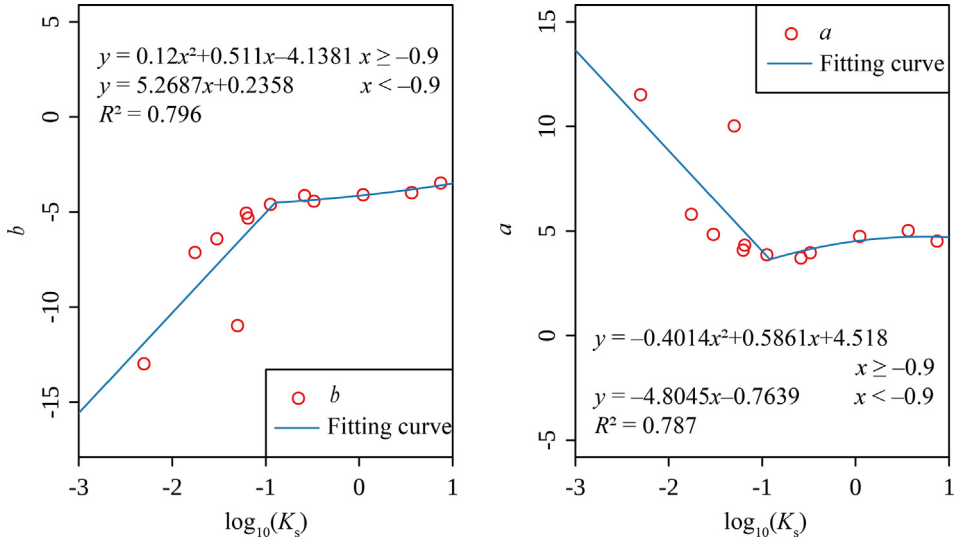

Fig. 3. The relationship between the logarithmic saturated hydraulic conductivity K_s and the two parameters of two piecewise lines obtained by fitting the hydraulic diffusivity curves of van Genuchten model in a semi-logarithmic coordinate system.

formula without empirical parameters α and n. As shown in Fig. 2, the empirical exponential function can reasonably describe the hydraulic diffusivity with the three physical meaning parameters, K_s, θ_s and θ_r.

2.4.3. Calculating correction term for heterogeneous soils

Soil water content is discontinuous at the material interface when a soil profile is heterogeneous (Hills et al., 1989; Khaleel et al., 2002; Zha et al., 2013; Matthews et al., 2005a, 2005b). Given that soil water content is a function of matric potential and soil hydraulic parameters, the vertical variation of θ in the gradational soil can be expressed as,

$$\frac{\partial\theta}{\partial z}=\frac{\partial\theta}{\partial h}\frac{\partial h}{\partial z}+\sum_{l=1}^{N}\frac{\partial\theta}{\partial p_l}\frac{\partial p_l}{\partial z}, \tag{23}$$

where p is a vector composed of N parameters, p_l (l = 1, 2, ...N), of the soil water retention function. This equation indicates that the vertical gradient of soil water content consists of two parts: the one caused by the vertical variation of h, and the other caused by the vertical variation of the parameters. Substituting Eq. (23) into Eq. (4), the diffusive term driven by the matric potential is,

$$\frac{\partial\theta}{\partial t}=\frac{\partial}{\partial z}\left(D(\theta)\left(\frac{\partial\theta}{\partial z}-\sum_{l=1}^{N}\frac{\partial\theta}{\partial p_l}\frac{\partial p_l}{\partial z}\right)\right). \tag{24}$$

There is an extra term $\sum_{l=1}^{N}\frac{\partial\theta}{\partial p_l}\frac{\partial p_l}{\partial z}$ on the right side of Eq. (24) compared to the equation in the homogeneous soil. This is a correction term to the gradient of soil water content for describing the soil variation due to heterogeneity. When adopting the van Genuchten model to represent the soil water characteristics, there are four parameters to describe the correction term, and they are the saturated water content θ_s (L^3L^{-3}), the residual water content θ_r (L^3L^{-3}), and two empirical parameters n (–) and α (L^{-1}). The analytical expressions of the partial derivative of soil water content with respect to each parameter are

$$\frac{\partial\theta}{\partial\theta_s}=[1+(-\alpha\times h)^n]^{-m}=S, \tag{25}$$

$$\frac{\partial\theta}{\partial\theta_r}=1-[1+(-\alpha\times h)^n]^{-m}=1-S, \tag{26}$$

$$\frac{\partial\theta}{\partial\alpha}=mnh(\theta_s-\theta_r)[1+(-\alpha h)^n]^{-m-1}(-\alpha h)^{n-1}, \tag{27}$$

$$\frac{\partial\theta}{\partial n}=(\theta_s-\theta_r)S\left[\frac{\ln(S)}{n(n-1)}-\frac{n-1}{n^2}(S^{n/1-n}-1)\ln(S^{n/1-n}-1)S^{-n/1-n}\right], \tag{28}$$

where S is the effective saturation (–). The four terms, $\frac{\partial\theta}{\partial\theta_s}$, $\frac{\partial\theta}{\partial\theta_r}$, $\frac{\partial\theta}{\partial\alpha}$, and $\frac{\partial\theta}{\partial n}$, of different soil types are shown in Fig. 4. The values of $\frac{\partial\theta}{\partial\theta_s}$ and $\frac{\partial\theta}{\partial\theta_r}$ can be easily calculated by using Eqs. (25) and (26) when effective saturation is obtained. The value of $\partial\theta/\partial\alpha$ is close to zero, which indicates that this item can be ignored in the correction term. Eq. (28) is complicated and requires parameter n. Since the values of n are not always available, a regression formula is developed to characterize the relationship between n with the saturated hydraulic conductivity K_s, as shown in Fig. 5. An exponential function is adopted as there is a strong positive correlation between K_s and n. As a result, parameter n can be calculated via

$$n=0.9509\times e^{0.72223\times\log_{10}(K_s)}+0.9. \tag{29}$$

Therefore, the diffusive term of the heterogeneous soil can be calculated with three parameters, which are the saturated hydraulic conductivity (K_s), the saturated water content (θ_s) and the residual water content (θ_r).

Considering all the three items (the advective term, source/sink term and the diffusive term) in our mass balance model, only four soil hydraulic parameters are essential to calculate the soil water movement, and they are the saturated hydraulic conductivity (K_s), the field capacity (θ_f), the saturated water content (θ_s) and the residual water content (θ_r). These parameters have physical mean-

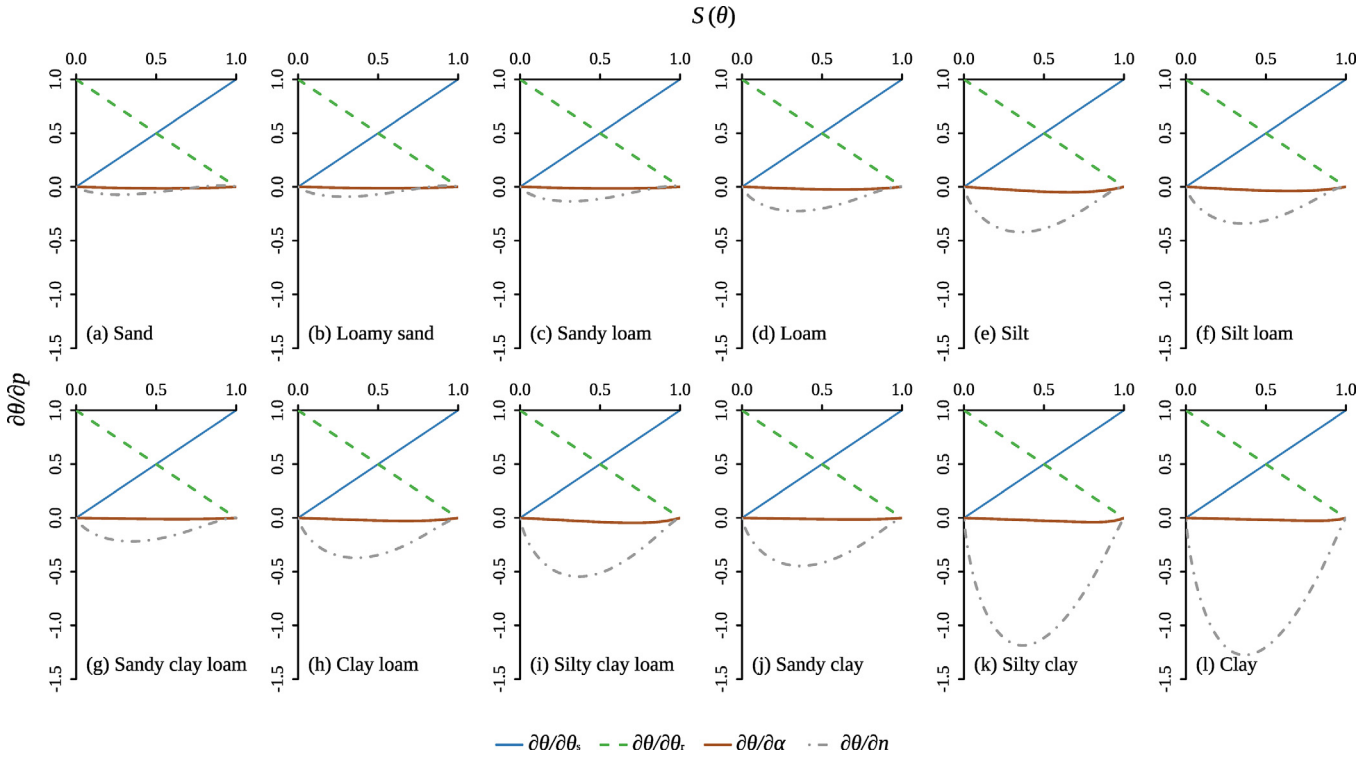

Fig. 4. The partial derivative of each parameter in the correction term for heterogeneous soils.

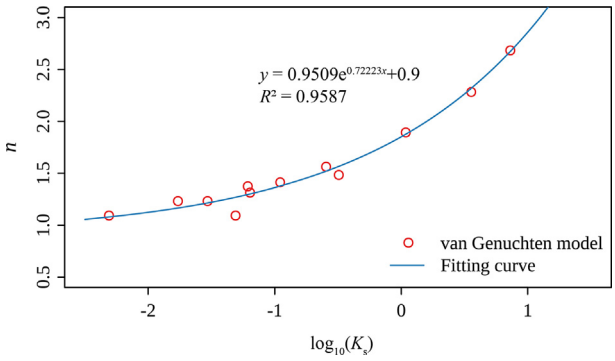

Fig. 5. The quadratic fitting between the saturated hydraulic conductivity and the empirical parameter *n*.

ings and are easy to be obtained, which makes the water balance model more applicable in practice. Furthermore, because of the implicit difference scheme used to discretize the diffusion equation, the water balance model is numerically stabile, and thus applicable to the simulations with coarse discretization in space and time.

3. Model evaluation and application

The water balance model is first tested by using two published infiltration cases with the homogeneous and heterogeneous soil conditions. Then three synthetic examples are designed to evaluate the model with different soil types, drainage functions, and discretization resolutions in space and time. The simulation results are compared with those obtained using HYDRUS-1D (Šimunek et al., 2008). The water balance model is also applied to a real-world lysimeter experiment with climate boundary conditions. For these cases, the mean absolute relative error (*ARE*) and the root mean squared error (*RMSE*) (Schoups et al., 2006; Zha et al., 2017) are used to quantitatively evaluate the misfit between the simulated results of the water balance model and HYDRUS-1D or observed water content. *ARE* and *RMSE* are calculated as,

$$ARE = \frac{1}{n}\sum_{i=1}^{n}\frac{|Y_i^j - H_i^j|}{H_i^j} \times 100\%, \tag{30}$$

$$RMSE = \sqrt{\frac{1}{n}\sum_{i=1}^{n}(Y_i^j - H_i^j)^2}, \tag{31}$$

where the subscript i represents the layer number and the superscript j represents the time level; Y_i^j is the simulated result of the proposed model and H_i^t is the observation or the results from HYDRUS-1D as the comparison standard.

3.1. Case 1: infiltration cases

Two published infiltration examples are used to test the performance of the model accuracy. The first one is a case with vertical infiltration in homogeneous soil based on the documentation of UNSATCHEM Module for HYDRUS (2D/3D) (Skagges et al., 1970; Šimůnek et al., 2012). The soil column is 0.6 m in length and filled with the sand with the saturated hydraulic conductivity of 0.6238 m/d. The column is subjected to ponded infiltration at the surface, and the bottom boundary is impermeable. The second example based on Hills et al. (1989) has heterogeneous soils with two soil types, Berino loamy fine sand and Glendale clay loam, whose saturated hydraulic conductivity are 5.41 m/d and 0.131 m/d, respectively. The soil column is 1 m in length, with each soil layer being 0.2 m in length. The constant infiltration rate is 0.02 m/d. The detailed information of the two examples can be found in references (Skagges et al., 1970; Šimůnek et al., 2012; Hills et al. 1989).

The water balance model is used to simulate the water content profiles under the two conditions, and the simulated results are compared with those from references as shown in Fig. 6. For the homogeneous example, the *ARE* values for the two profiles at times 3600 s and 7200 s (Fig. 6 (a) and (b)) are 22% and 12%, and the *RMSE* values are 0.088 cm^3/cm^3 and 0.044 cm^3/cm^3. The percentage error of the mass balance is 3×10^{-6} for the water balance model. For the second heterogeneous example, the *ARE* values for the two profiles at times 1d and 5d (Fig. 6(c) and (d)) are 6.6% and 13.6%, and the *RMSE* values are 0.025 cm^3/cm^3 and 0.045 cm^3/cm^3. The percentage error of the mass balance is 5×10^{-6} for the water balance model. The comparison results of the two examples show that the water balance

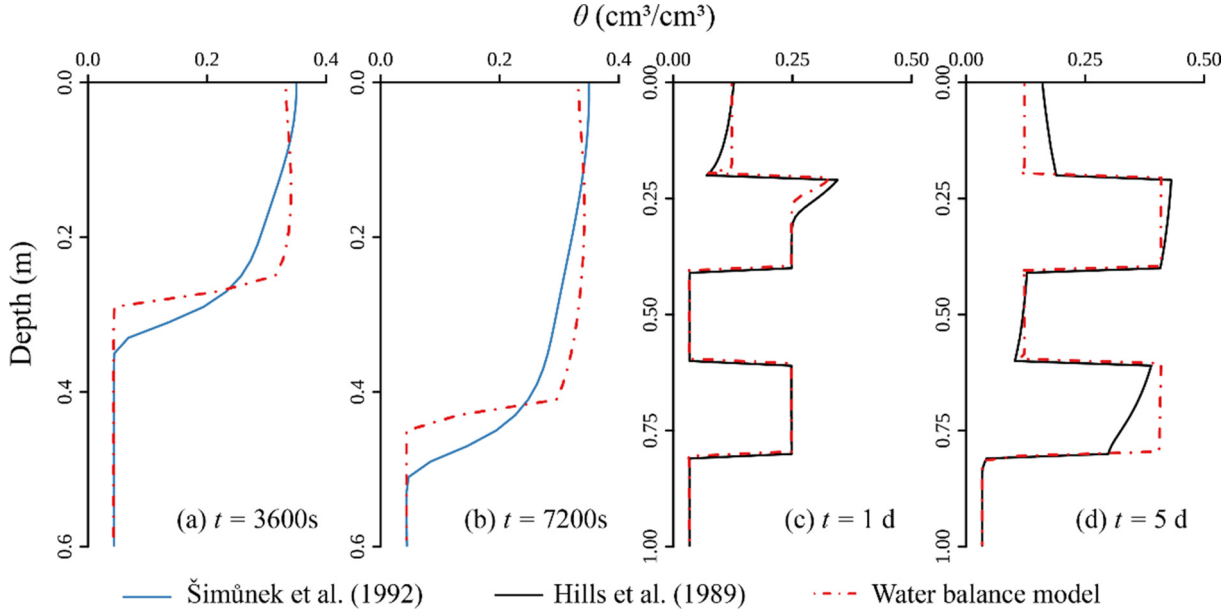

Fig. 6. Water content profiles at various times from the water balance model and the results from references.

Table 2
The soil hydraulic parameters for different soil types.

Soil type	The parameters used both by the proposed model and HYDRUS-1D			The parameter used only by the proposed model	The parameters used only by HYDRUS-1D	
	θ_r (cm^3/cm^3)	θ_s (cm^3/cm^3)	K_s (m/d)	θ_f (cm^3/cm^3)	α (1/m)	n (–)
Sand	0.045	0.43	7.128	0.08	14.5	2.68
Loamy sand	0.057	0.41	3.502	0.12	12.4	2.28t
Loam	0.078	0.43	0.2496	0.27	3.6	1.56
Silt loam	0.067	0.45	0.108	0.3	2	1.41
Clay loam	0.095	0.41	0.0624	0.33	1.9	1.31
Sandy clay	0.1	0.38	0.0288	0.35	2.7	1.23
Silty clay	0.07	0.36	0.0048	0.37	0.5	1.09
Clay	0.068	0.38	0.048	0.39	0.8	1.09

model can capture the characteristic of the infiltration process and keep water balance well both for the homogeneous and heterogeneous soils.

3.2. Case 2: soil water movement driven by matric potential with various soil types

In this numerical example, the developed water balance model is used to simulate the soil water movement driven by the matric potential, and the main purpose is to evaluate the accuracy of the simplified method for describing the diffusive term as shown in Section 2.4.2. The soil column is 2 m in length, and the profile is homogeneous, with both the top and bottom boundaries being impermeable. The initial soil water content of the top half profile is set as 0.15, and the bottom half profile as 0.35. Eight types of soils with the soil hydraulic parameters and the field capacity given by Carsel and Parrish (1988) and Ratliff et al. (1983) are listed in Table 2. The linear drainage function is used in the water balance model. The spatial discretization resolution of HYDRUS-1D and the water balance model are both 2 cm, and the time step of the water balance model is a constant value of 0.5 day, which is close to the mean time step of HYDRUS-1D.

The water balance model is used to simulate the water movement, and the simulated soil water content profiles for the different soil types at the 30th day are compared with those of HYDRUS-1D, as shown in Fig. 7. The soil water content in the top half profile increases over time. The increased soil water content is driven by the matric potential, since the water movement under gravitational potential is downward. The good match of the soil water content in the top half profile of the two models indicates that the water balance model can calculate the upward flow satisfactorily, especially for loam and clay. We list the *ARE* values and the *RMSE* values of the profiles in Table 3. The *ARE* values are less than 11%, and the *RMSE* values are less than 0.05 cm^3/cm^3, which indicate that the simplify method of diffusivity can reasonably simulate the upward flow driven by matric potential.

Fig. 7 shows that there is relative poor performance in the bottom half profile where the soil water content near the saturated water content for loam, silty loam and clay loam soils. The reason is that, in the bottom half profile, the gravitational potential and the matric potential simultaneously drive the soil movement as the soil water content in this region exceeds the field capacity, whereas the water balance model considers the two forces separately, first calculating the downward flow driven by the gravitational potential and then calculating the upward flow driven by the matric potential. In other words, the model may overestimate the upward flux near the water table, which leads to an underestimation of soil water content below water table and an overestimation of soil water content above water table.

Generally speaking, this numerical example indicates that the simplify method of diffusivity can reasonably simulate the upward flux driven by the matric potential, despite that the water balance model may overestimate the upward flux near a water table. Furthermore, the average simulation time of HYDRUS-1D is 0.22 s, larger than that for the water balance model (Table 3), which indicates that the water balance model is 3 to 10 times faster than HYDRUS-1D. The percentage error of mass balance is in the order of magnitude of 10^{-4} for HYDRUS-1D but 10^{-7} for the water balance model. These indicate that the water balance model is more efficient with better water balance.

3.3. Case 3: soil water movement with complicated boundary and estimation of drainage functions

This numerical example is to evaluate the performance of the water balance model under complex boundary conditions, such as under the variable atmospheric boundary condition. The numerical example also evaluates the performance of the water balance model for the drainage functions listed in Table 1. The soil column of this example is 2 m in length. There is no crop on the top boundary, and the bottom boundary is impermeable. Fig. 8 shows the top boundary condition, including the daily precipitation and the soil evaporation. The annual precipitation is 650 mm, and the annual soil evaporation is 756 mm. The initial water table is in the depth of 0.48 m, and the soil water content changes linearly from 0.2 at the surface to saturation at the water table. The soil is loam with the soil hydraulic parameters and the field capacity listed in Table 2. The spatial discretization of HYDRUS-1D and the water balance model are both 2 cm, and the time step of the water balance model is 0.1 day, which is close to the mean time step of HYDRUS-1D.

The soil water content profiles at different times of the water balance model with the 5 drainage functions are compared with those of HYDRUS-1D, as shown in Fig. 9. The results show that the water balance model can simulate the vertical flow satisfactorily. The mean *RMSE* values and *ARE* values of the 5 drainage functions are listed in Table 4. All the *RMSE* values are less than 0.02 m^3/m^3, and the *ARE* values are less than 4%, which indicate a good performance of the water balance model. Specifically speaking, the exponential, power and square drainage functions have lower *RMSE* values and *ARE* values than the other functions.

The mean soil water content at the depth of 0–10 cm between the water balance model with 5 drainage functions and HYDRUS-1D are compared in Fig. 10. The domain volume is used as the weight to average the water content of nodes within the depth of 0–10 cm to obtain the mean water content of HYDRUS-1D. It shows that the water content calculated by the water balance model has the similar trend with those obtained using HYDRUS-1D, but fluctuates more abruptly when the infiltration water or evapotranspiration is directly added to or subtracted from each soil layer, while the soil water content in HYDRUS-1D changes more smoothly. The calculated mean soil water content at the depth of 0–10 cm by the water balance model are smaller than the values calculated by HYDRUS-1D during the first 50 days. This difference

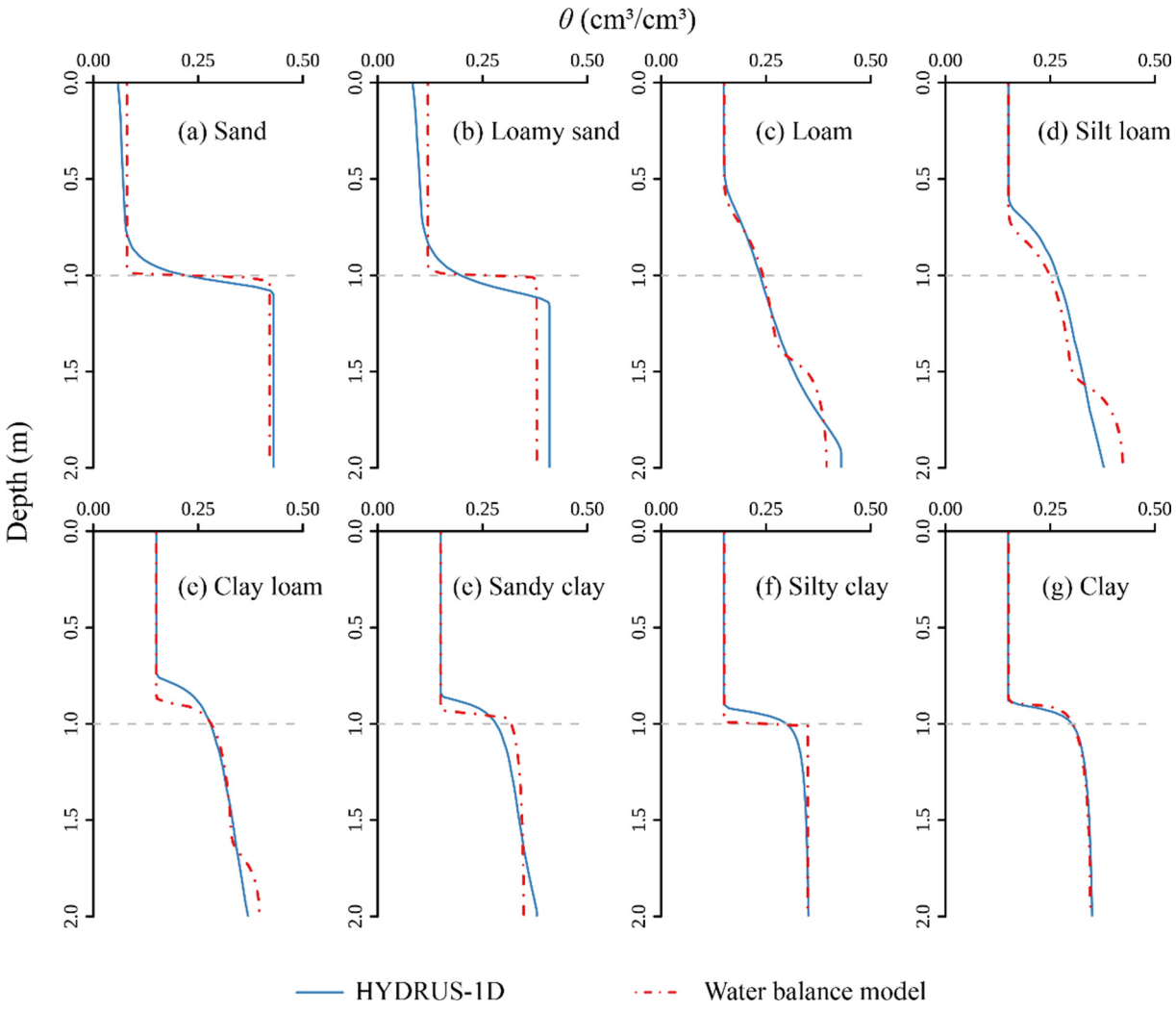

Fig. 7. Comparison of the soil water content profiles between the water balance model and HYDRUS-1D for different soil types at the 30th day.

Table 3
The *ARE* values, *RMSE* values, calculation times of HYDRUS-1D and the water balance model for each soil type of case 2.

Soil type	*ARE* (%)	*RMSE* (cm^3/cm^3)	HYDRUS-1D calculation time (s)	Water balance model calculation time (s)
Sand	10.4	0.043	0.26	0.016
Loamy sand	9.5	0.046	0.25	0.016
Loam	4.1	0.015	0.14	0.031
Silt loam	9.3	0.032	0.16	0.047
Clay loam	4.2	0.021	0.27	0.063
Sandy clay	4.3	0.017	0.21	0.063
Silty clay	2.3	0.017	0.24	0.063
Clay	2.3	0.014	0.24	0.063

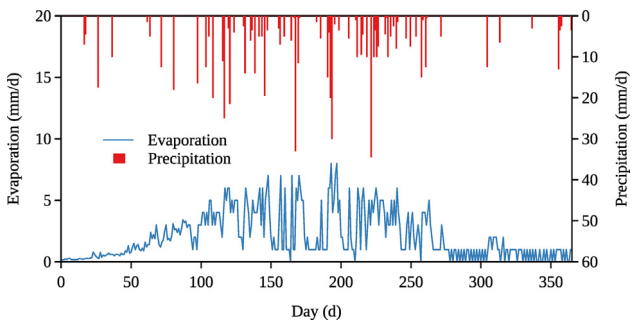

Fig. 8. Daily precipitation and soil evaporation of the top boundary condition.

is attributed to the use of the drainage function when the soil water content ranges from the field capacity (θ_f) to the saturated water content (θ_s) in the water balance model. Fig. 11 shows the relationship between soil water content and unsaturated hydraulic conductivity of the van Genuchten model and the 5 drainage functions. The water balance model has larger unsaturated hydraulic conductivities calculated by the 5 drainage functions when the soil water content exceeds the layer's field capacity. As a result, the water balance model may overestimate the infiltration when the infiltration is more than the evapotranspiration during the first 50 days, and gives smaller soil water content in the top layer. During the period from the 200th day to the 300th day, the surface soil water content fluctuates more drastically as the influence of the

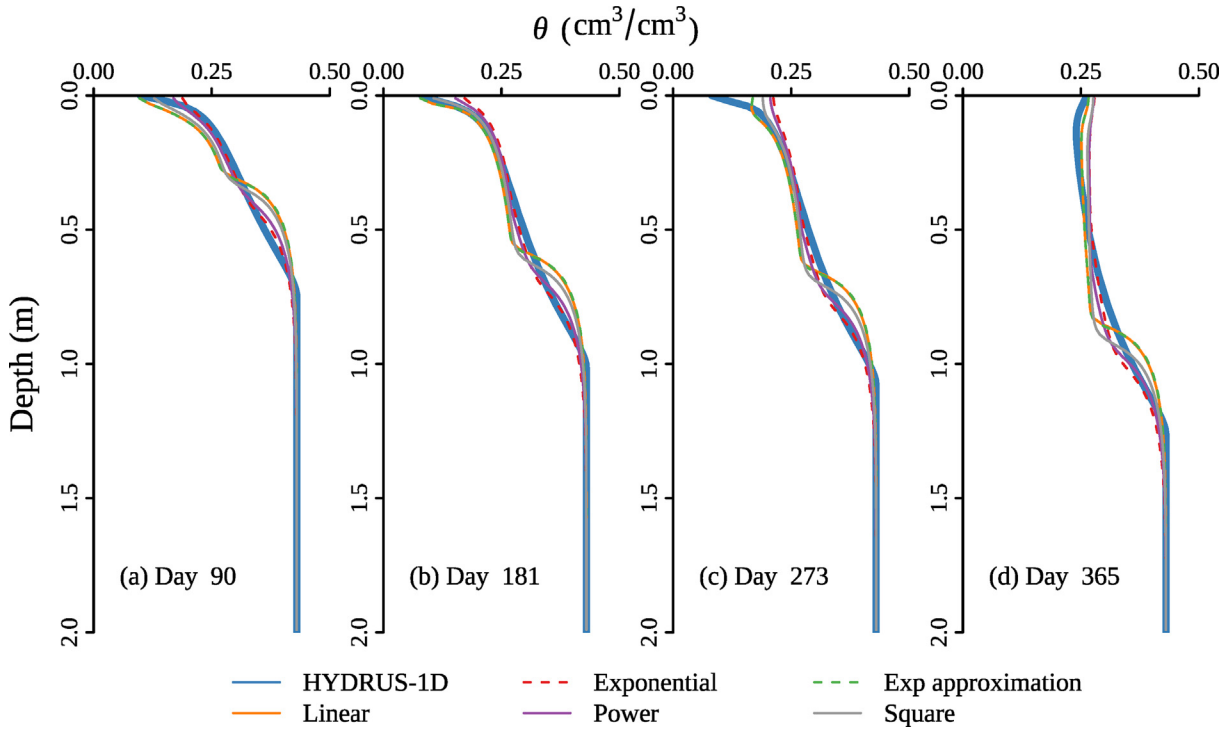

Fig. 9. Comparison of the soil water content profiles between the water balance model with 5 drainage functions and HYDRUS-1D at different times.

Table 4
The mean *RMSE* and *ARE* values of soil water content between the water balance model with 5 drainage functions and HYDRUS-1D.

	RMSE (cm^3/cm^3)	*ARE* (%)
Linear	0.018	3.7
Exponential	0.013	2.8
Power	0.012	2.8
Exp approximation	0.019	3.8
Square	0.016	3.4

top boundary (Fig. 10). The exponential drainage function overestimates the soil water content, while the linear and exponential approximation drainage functions underestimate the soil water content. The power and square drainage functions give more accurate results. A comprehensive consideration of the performance of each drainage function leads to the conclusion that, for the water balance model, the power drainage function and square function

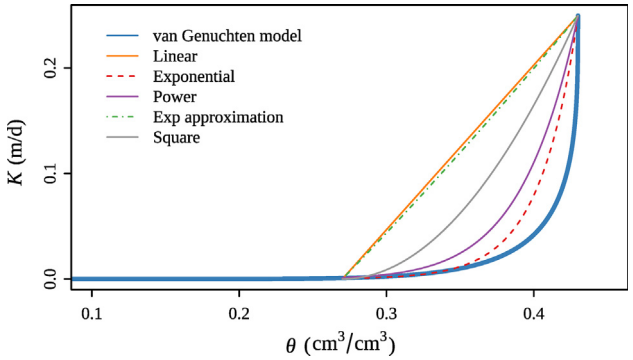

Fig. 11. The unsaturated hydraulic conductivity curves of van Genuchten model and the 5 drainage functions.

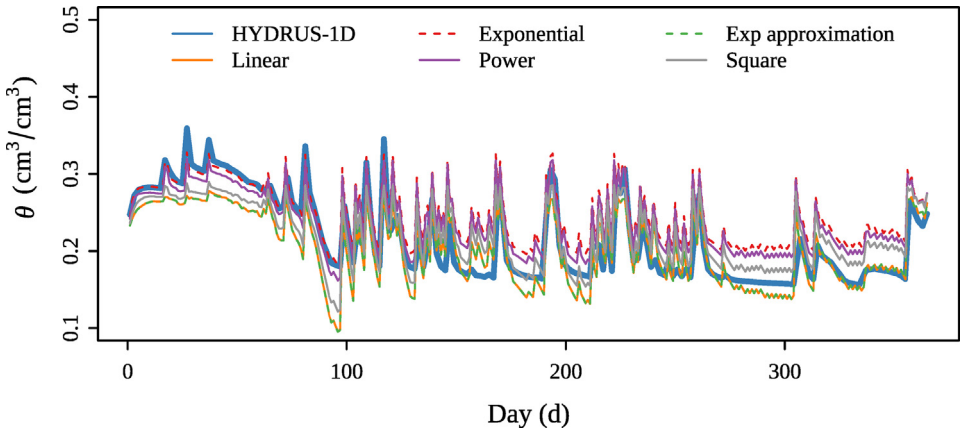

Fig. 10. Comparison of the mean soil water content of 0–10 cm between the water balance model with 5 drainage functions and HYDRUS-1D.

are recommended, due to their satisfactory performance in terms of *RMSE* values and *ARE* values and the smaller number of parameters.

The simulation times of HYDRUS-1D and the water balance model are 3.5 s and 2 s respectively, which indicates that the water balance model is almost 2 times faster than HYDRUS-1D. The percentage error of the mass balance is in the order of magnitude of 10^{-3} for HYDRUS-1D but10^{-4} for the water balance model. In general, the water balance model is effective and efficient for simulating the water movement in the unsaturated zone under complex top boundary conditions. The square function and the power function are chosen as the recommend drainage functions.

3.4. Case 4: soil water movement in heterogeneous soils with various spatial discretization and time steps

In this example, heterogeneous soils with complicated boundary conditions are considered to evaluate the performance of the water balance model with different discretization resolutions in space and time. The soil column is 2 m in length, filled with alternating layers of two types of soil (each layer being 0.4 m thick). The two soil types are sandy loam and silt loam, and the filling starts with silt loam in the first layer. The soil hydraulic parameters and field capacity are listed in Table 2. The top boundary is the atmospheric boundary, and the bottom boundary is impermeable. Fig. 12 plots the daily precipitation and soil evaporation of the top boundary. The annual precipitation is 650 mm, and the annual soil evaporation is 672.01 mm. The initial soil water content is uniform with the value of 0.25. The square drainage function is used in the water balance model.

In order to evaluate the model applicability to various spatial discretization and time steps under the heterogeneous soil, eight modeling scenarios with the spatial discretization and time steps 10 cm 1 h, 10 cm 1d, 20 cm 1 h, 20 cm 1d, 20 cm 2d, 20 cm 5d, 20 cm 10d and 20 cm 15d are used by the water balance model. The HYDRUS-1D model with spatial resolution of 2 cm are adopted as a reference.

The simulated soil water content profiles of the eight scenarios are compared with those from HYDRUS-1D as shown in Fig. 13. The *RMSE* values, *ARE* values, and mass balance errors are listed in Table 5. All the scenarios can simulate mass balance well with the percentage mass balance error as being 10^{-5} or less. The first five scenarios obtain very similar results with satisfactory performance in the first, third and fifth soil layers, as the *RMSE* values are less than 0.041 cm^3/cm^3 and *ARE* values less than 10.4%. The *ARE* values of the second and the fourth layers increase significantly. It is caused by the smaller value of soil water content in the two layers of sandy loam, which has smaller water holding capacity and soil water content. However, the *RMSE* values of the second and the fourth layers are close to 0.04 cm^3/cm^3, which indicate an acceptable result. When we keep the spatial step at 20 cm and increase the time step from 2d, 5d, 10d to 15d, the *RMSE* values and *ARE* values become worse, especially for the top layers. The result of the scenario with the time step of 5d is acceptable. However, when the time step increases to 10d or 15d, the mean *ARE* value over the five layers is more than 20% and the mean *RMSE* value over the five layers is close to 0.05 cm^3/cm^3, which indicates that the results of simulated soil water content are not acceptable. The reason is that, for a small time step, the amount of infiltration is small and limited to the top layers only; this water can be removed from the soil layers by evapotranspiration, and thus does not reach deeper layers quickly. This is similar to what happens in the real case. However, when the time step is large, the amount of infiltration becomes large enough to reach deeper soil layers before the infiltration water is removed by evapotranspiration, which leads to smaller soil water content at top layers but larger soil content in deeper layers. Therefore, the simulated soil water content with a large time step are unacceptable.

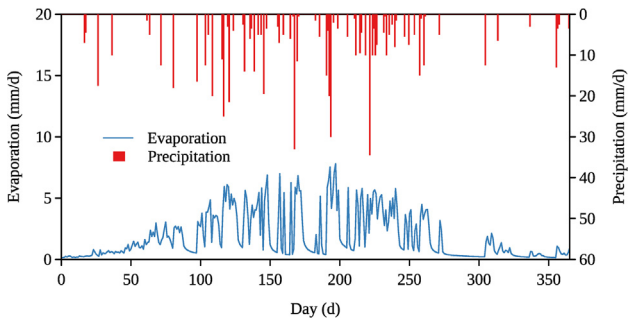

Fig. 12. Daily precipitation and soil evaporation of the top boundary condition.

Generally speaking, when the time steps are less than 5 days, there will be a proper accuracy of the soil water content. Furthermore, it is found that, for the water balance model, the accuracy of is similar for all the first five scenarios, which indicates that the water balance model yields satisfactory results even for the scenarios with large spatial discretization and time steps under heterogeneous soil conditions with complicated boundary conditions.

3.5. Case 5: real-world application to lysimeter experiment

The lysimeter experiment was conducted from November 2003 to June 2004 during the growing season of winter wheat in Irrigation and Drainage Experiment Station at Wuhan University, China (Wang, 2007; Zhu et al., 2009, 2017). The size of the lysimeter is 2 m × 2 m × 3 m. The evapotranspiration was not directly measured, and a value of 75 percent of annual mean water requirement of the crop growth is used in this simulation. The crop transpiration rate over the soil evaporation rate is assumed to be 3:1 during the crop growing season. Fig. 14 plots the precipitation/irrigation rate, the crop transpiration rate, and the soil evaporation rate. The bottom boundary is set as the free drainage condition. The soil hydraulic parameters of the lysimeter experiment used in the water balance model are listed in Table 6. The time step is 1 h and the spatial step is 10 cm in the water balance model.

The simulated cumulative evaporation and transpiration are 94.2 mm and 282.7 mm, respectively, and the simulated flux at the bottom of the lysimeter is 73.7 mm. The percentage error of the mass balance for the water balance model is in the order of magnitude of 10^{-4}. Fig. 15 shows the comparison of simulated and observed soil water content at different times. The *RMSE* values of each profile are 0.008 cm^3/cm^3, 0.021 cm^3/cm^3, 0.013 cm^3/cm^3 and 0.014 cm^3/cm^3, respectively. And the *ARE* values are 2.1%, 6.5%, 3.1% and 4.7%, respectively, which indicate a good performance of the water balance model. Fig. 16 shows the comparison of the simulated and observed soil water content over time at different observation layers. The soil water content at the depth of 0.1 m fluctuates drastically due to the influence of the top boundary condition. The water balance model has a good fit with the observed data except during the time between the 80th day and the 130th day. The reason is that, the evaporation and transpiration of the top boundary may insufficient to reduce the top soil water content since the mean seasonal value is used. At the depth of 0.7 m, the water balance model has a good performance. While at the depth of 1.3 m and 1.7 m, the water balance model shows sharp increases of the water content, and this is caused by the assumption that the infiltration water is allocated instantaneously after irrigation or precipitation. Overall, the performance of the water balance model is satisfactorily.

When using different spatial discretization resolution and time steps, the observed soil water content and the simulated

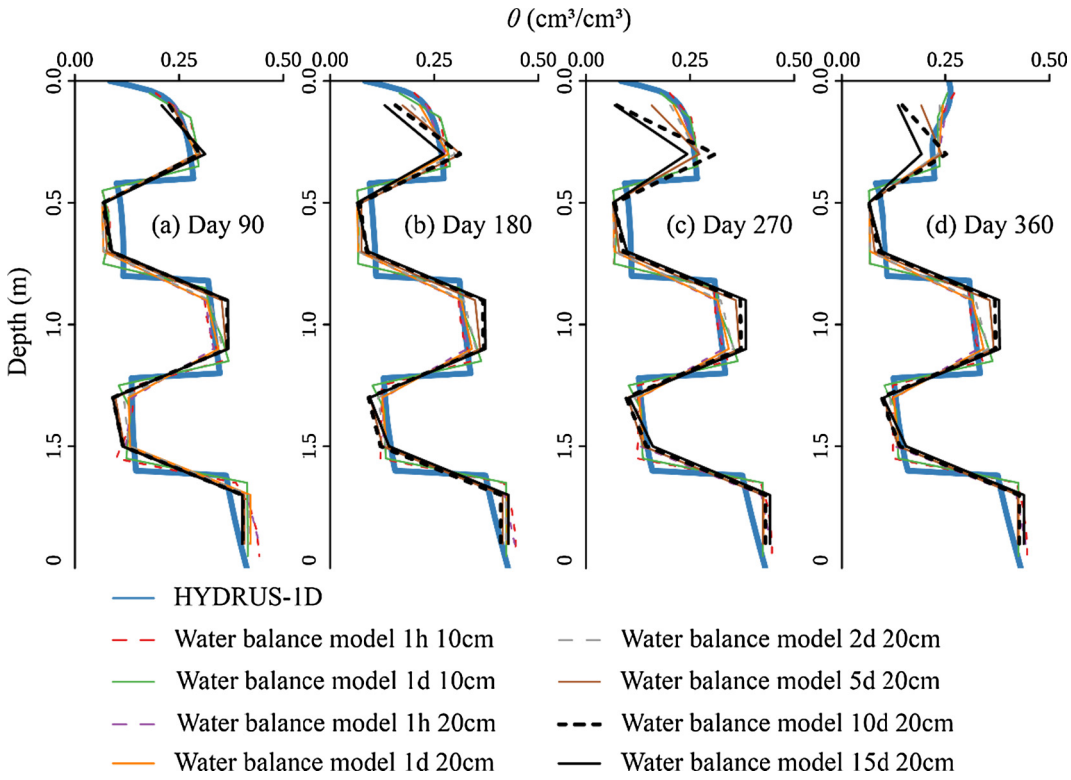

Fig. 13. The comparison of the simulated results of the proposed water balance model with different spatial and time steps with the results from HYDRUS-1D.

Table 5
The *RMSE* values and *ARE* values of the five soil texture layers with different spatial discretization and time steps.

Spatial and time steps		First layer	Second layer	Third layer	Forth layer	Fifth layer	Mass balance error (%)
10 cm, 1 h	*RMSE* (cm^3/cm^3)	0.020	0.039	0.011	0.024	0.041	5.8×10^{-5}
	ARE (%)	6.7	32.5	3.1	14.3	10.2	
10 cm, 1 d	*RMSE* (cm^3/cm^3)	0.020	0.039	0.019	0.028	0.038	1.8×10^{-5}
	ARE (%)	6.9	33.0	5.2	14.5	8.6	
20 cm, 1 h	*RMSE* (cm^3/cm^3)	0.014	0.041	0.005	0.018	0.041	3.9×10^{-5}
	ARE (%)	5.3	35.6	1.5	12.0	10.4	
20 cm, 1 d	*RMSE* (cm^3/cm^3)	0.014	0.041	0.011	0.016	0.040	2.2×10^{-5}
	ARE (%)	4.9	35.4	3.2	10.5	9.6	
20 cm, 2 d	*RMSE* (cm^3/cm^3)	0.018	0.040	0.019	0.023	0.039	9.9×10^{-6}
	ARE (%)	6.7	35.0	5.9	14.5	9.1	
20 cm, 5 d	*RMSE* (cm^3/cm^3)	0.038	0.037	0.041	0.036	0.034	1.3×10^{-5}
	ARE (%)	14.3	31.7	12.6	22.7	7.8	
20 cm, 10 d	*RMSE* (cm^3/cm^3)	0.067	0.032	0.050	0.039	0.034	9.8×10^{-6}
	ARE (%)	26.7	27.0	15.5	23.8	7.8	
20 cm, 15 d	*RMSE* (cm^3/cm^3)	0.079	0.032	0.059	0.035	0.040	1.4×10^{-6}
	ARE (%)	28.6	25.1	18.2	21.4	9.48	

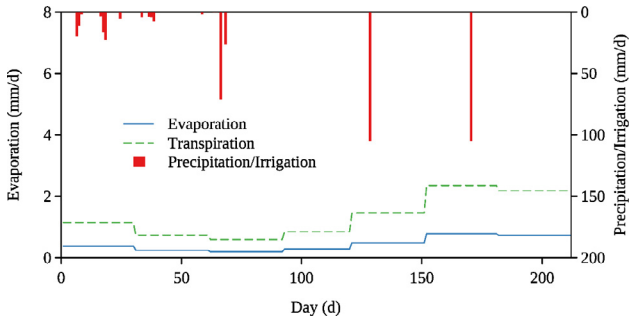

Fig. 14. The top boundary conditions of daily evaporation rate, daily transpiration rate and daily precipitation and irrigation rate.

results of HYDRUS-1D and the water balance model over time at different layers are compared in Fig. 16. The percentage error of the mass balance, the mean *RMSE* values, the mean *ARE* values and the computational costs of the water balance model and HYDRUS-1D are shown in Table 7. When the time step increases from 1 h to 1d and the spatial discretization increases from 10 cm to 20 cm, the proposed model can still simulate the observations well. The *ARE* and *RMSE* do not show worse trend. The model also can simulate mass balance well with the percentage error of the mass balance remained as 10^{-5}. The results indicate that the water balance model is suitable for the large spatial discretization and time steps. This however is not the case for HYDRUS-1D. While HYDRUS-1D has good results at the time

Table 6
The soil parameters of the lysimeter experiment.

Depth	θ_r (cm^3/cm^3)	θ_s (cm^3/cm^3)	θ_f (cm^3/cm^3)	K_s (m/d)
0–0.2m	0.067	0.45	0.25	0.74
0.2–1.6m	0.1	0.39	0.33	0.53
1.6–3m	0.068	0.38	0.38	0.14

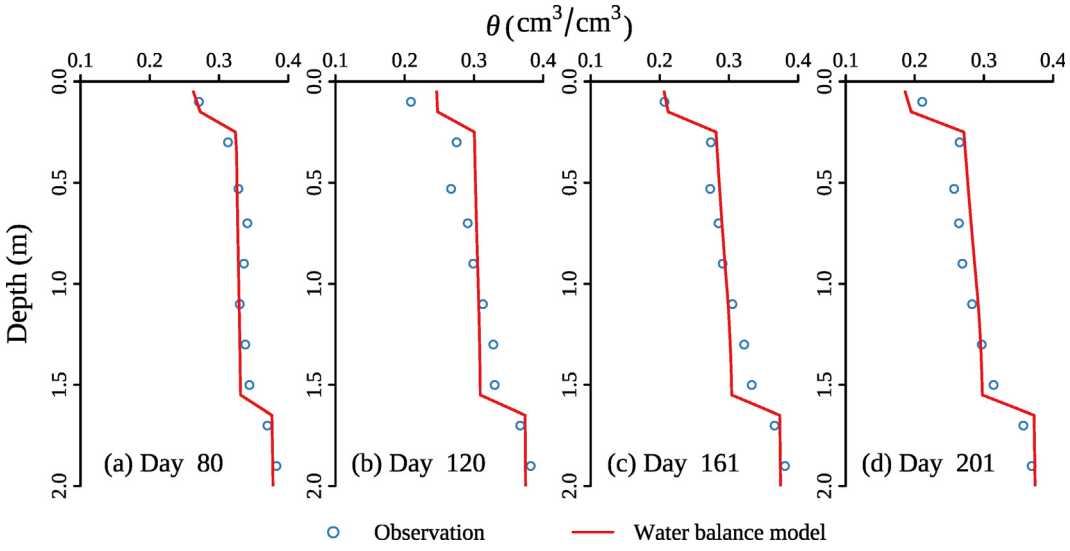

Fig. 15. Comparison of the soil water content profiles between the water balance model and observed data at different times for the practical lysimeter experiment.

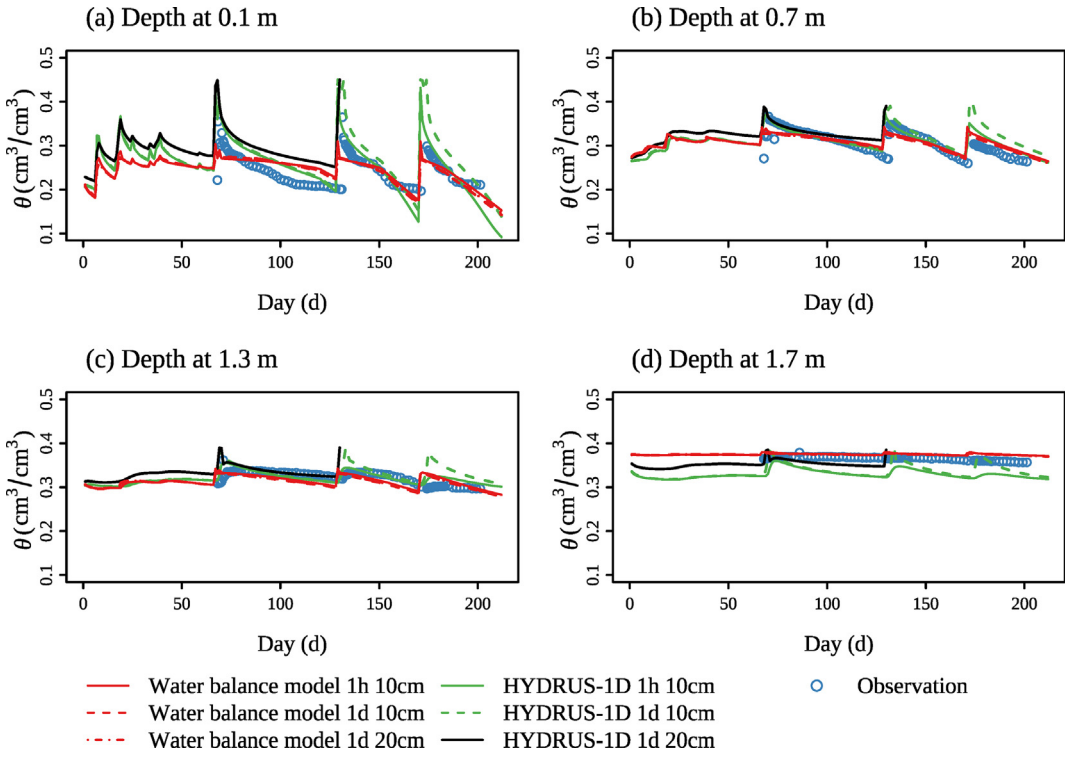

Fig. 16. The comparison of the observed soil water content, the simulated results of HYDRUS-1D and the proposed water balance model over time at different soil depths with different spatial discretization and time steps.

step of 1 h and spatial discretization of 10 cm, the simulation results deteriorate with the increased spatial discretization and time steps. The HYDRUS-1D results are unreasonable in that the soil becomes saturated after the 130th day when the time step of 1 d and spatial discretization of 20 cm, which is caused by the intensive irrigation that leads to an iterative error. Additionally, the water balance model is more effective than HYDRUS-1D as shown in Table 7, and the simulation times indicate the computation efficiency of the water balance model is 2 to 4 times faster.

Table 7
The percentage error of the mass balance, the *RMSE* and *ARE* values of the water balance model and HYDRUS-1D with different spatial discretization and time steps.

	Water balance model			HYDRUS-1D		
	1 h 10 cm	1 d 10 cm	1 d 20 cm	1 h 10 cm	1 d 10 cm	1 d 20 cm
Mass balance error (%)	9×10^{-6}	9×10^{-6}	1×10^{-5}	0.19	4.35	–
RMSE (cm^3/cm^3)	0.0175	0.0175	0.0173	0.019	0.029	–
ARE (%)	4.83	4.76	4.72	5.26	8.15	–
Computational time (s)	0.30	0.11	0.09	1.25	0.25	–

As a summary, the results shown in Figs. 15 and 16 indicate that the simulated soil water content of the water balance model has a satisfactory agreement with the observed data. And the water balance model can be used for coarse spatial discretization and large time steps.

4. Conclusions

This study develops a one-dimensional water balance model with physically meaningful parameters for simulating vertical water movement in unsaturated soils. The model can effectively and efficiently capture the features of soil water movement. The model is evaluated by using both synthetic numerical examples and real-world experimental data. The major conclusions drawn from this research are as follows:

(1) The water balance model can simulate both upward and downward flow in the unsaturated zone by considering the advective term driven by the gravitational potential, the source/sink term, and the diffusive term driven by the matric potential individually. The model yields satisfactory mass balance even for coarse spatial discretization and large time step, which greatly improves the efficiency and applicability of the model.
(2) When solving the advective soil movement, the water balance model is compatible with various drainage functions used to describe the relationship between unsaturated hydraulic conductivity and soil water content. The square drainage function and the power drainage function are superior to other functions due to their satisfactory performance and with no empirical parameters.
(3) A new empirical formula is developed to calculate the diffusivity with three parameters (the saturated hydraulic conductivity, the saturated water content and the residual water content). When solving the diffusive soil movement in the heterogeneous soil, a correction term is used and evaluated using the simplified function with the three parameters above.
(4) Applying the water balance model to simulation soil water movement in the unsaturated zone demonstrates the accommodation of the model to the upward flow, complex boundary conditions, and soil heterogeneity conditions.
(5) The water balance model may overestimate the upward flux close to water table, due to the equations for advective flow, source/sink term, and diffusive flow solved separately.

Acknowledgments

The study was partially supported by the National Key Research and Development Program of China (2016YFC0501304), and Natural Science Foundation of China through Grants (51479143, 51779178, 51629901).

References

Abedinpour, M., Sarangi, A., Rajput, T.B.S., Singh, M., 2014. Prediction of maize yield under future water availability scenarios using the AquaCrop model. J. Agric. Sci. 152 (4), 558–574.
Abeysingha, N.S., Singh, M., Sehgal, V.K., Khanna, M., Pathak, H., Jayakody, P., Srinivasan, R., 2015. Assessment of water yield and evapotranspiration over 1985–2010 in the Gomti River basin in India using the SWAT model. Curr. Sci. 108 (12), 2202–2212.
Adnan, A.A., Jibrin, J.M., Kamara, A.Y., Abdulrahman, B.L., Shaibu, A.S., Garba, I.I., 2017. CERES-maize model for determining the optimum planting dates of early maturing maize varieties in Northern Nigeria. Front. Plant Sci. 8. https://doi.org/10.3389/fpls.2017.01118.
Allen, R.G., Pereira, L.S., Raes, D., Smith, M., 1998. Crop Evapotranspiration-Guidelines For Computing Crop Water Requirements-FAO Irrigation and Drainage Paper No. 56. Food and Agriculture Organisation, Italy.
Arnold, J.G., Moriasi, D.N., Gassman, P.W., Abbaspour, K.C., White, M.J., Srinivasan, R., Santhi, C., Harmel, R.D., van Griensven, A., Van Liew, M.W., Kannan, N., Jha, M.K., 2012. SWAT: model use, calibration, and validation. Trans. ASABE 55 (4), 1491–1508.
Bastiaanssen, W.G.M., Allen, R.G., Droogers, P., D'Urso, G., Steduto, P., 2007. Twenty-five years modeling irrigated and drained soils: state of the art. Agric. Water Manage. 92 (3), 111–125.
Bellot, J., Chirino, E., 2013. Hydrobal: an eco-hydrological modelling approach for assessing water balances in different vegetation types in semi-arid areas. Ecol. Model. 266, 30–41.
Berengena, J., Gavilan, P., 2005. Reference evapotranspiration estimation in a highly advective semiarid environment. J. Irrig. Drain. Eng. 131 (2), 147–163.
Braud, I., Varado, N., Olioso, A., 2005. Comparison of root water uptake modules using either the surface energy balance or potential transpiration. J. Hydrol. 301, 267–286.
Carsel, R.F., Parrish, R.S., 1988. Developing joint probability distributions of soil water retention characteristics. Water Resour. Res. 24 (5), 755–769.
Carsel, R.F., Parrish, R.S., Jones, R.L., Hansen, J.L., Lamb, R.L., 1988. Characterizing the uncertainty of pesticide leaching in agricultural soils. J. Contam. Hydrol. 2 (2), 111–124.
Dai, J.F., Cui, Y.L., Cai, X.L., Brown, L.C., Shang, Y.H., 2016. Influence of water management on the water cycle in a small watershed irrigation system based on a distributed hydrologic model. Agric. Water Manage. 174, 52–60.
Diersch, H.J., 2013. FEFLOW: Finite Element Modeling of Flow, Mass and Heat Transport in Porous and Fractured Media. Springer Science & Business Media, Berlin Heideberg.
Downer, C.W., Ogden, F.L., 2004. Appropriate vertical discretization of Richards' equation for two-dimensional watershed-scale modelling. Hydrol. Process. 18, 1–22.
FILL, V., 2008. Documentation of Computer Program INFIL3.0-A Distributed-Parameter Watershed Model to Estimate Net Infiltration Below the Root Zone. U.S. Geological Survey. Scientific Investigation Report 2008-5006, Online only, http://pubs.usgs.gov/sir/2008/5006/pdf/SIR2008-5006.pdf.
Gandolfi, C., Facchi, A., Maggi, D., 2006. Comparison of 1D models of water flow in unsaturated soils. Environ. Modell. Softw. 21 (12), 1759–1764.
Graham, D.N., Butts, M.B., 2005. Flexible, integrated watershed modelling with MIKE SHE. In: Singh, V.P., Frevert, D.K. (Eds.), Watershed Models. Water Resources Publication, Highlands Ranch, Colorado. ISBN 0849336090.
Gu, C.H., Riley, W.J., 2010. Combined effects of short term rainfall patterns and soil texture on soil nitrogen cycling-a modeling analysis. J. Contam. Hydrol. 112 (1), 141–154.
Hayek, M., 2016. An exact explicit solution for one-dimensional, transient, nonlinear Richards' equation for modeling infiltration with special hydraulic functions. J. Hydrol. 535, 662–670.
Hills, R.G., Porro, I., Hudson, D.B., Wierenga, P.J., 1989. Modeling one-dimensional infiltration into very dry soils: 1. Model development and evaluation. Water Resour. Res. 25 (6), 1259–1269.
Holzworth, D.P., Huth, N.I., deVoil, P.G., Zurcher, E.J., Herrmann, N.I., McLean, G., Chenu, K., van Oosterom, E.J., Snow, V., Murphy, C., Moore, A.D., Brown, H., Whish, J.P.M., Verrall, S., Fainges, J., Bell, L.W., Peake, A.S., Poulton, P.L., Hochman, Z., Thorburn, P.J., Gaydon, D.S., Dalgliesh, N.P., Rodriguez, D., Cox, H., Chapman, S., Doherty, A., Teixeira, E., Sharp, J., Cichota, R., Vogeler, I., Li, F.Y., Wang, E., Hammer, G.L., Robertson, M.J., Dimes, J.P., Whitbread, A.M., Hunt, J., van Rees, H., McClelland, T., Carberry, P.S., Hargreaves, J.N.G., MacLeod, N., McDonald, C., Harsdorf, J., Wedgwood, S., Keating, B.A., 2014. APSIM-Evolution towards a new generation of agricultural systems simulation. Environ. Modell. Softw. 62, 327–350.
Householder, A.S., 2006. The Theory of Matrices in Numerical Analysis. Dover Publications, New York.
Huth, N.I., Bristow, K.L., Verburg, K., 2012. SWIM3: model use, calibration, and validation. Trans. ASABE 55 (4), 1303–1313.
Jiang, J., Zhang, Y., Wegehenkel, M., Yu, Q., Xia, J., 2008. Estimation of soil water content and evapotranspiration from irrigated cropland on the North China Plain. J. Plant Nutr. Soil Sci. 171, 751–761.

Jones, J.W., Hoogenboom, G., Porter, C.H., Boote, K.J., Batchelor, W.D., Hunt, L.A., Wilkens, P.W., Singh, U., Gijsman, A.J., Ritchie, J.T., 2003. The DSSAT cropping system model. Eur. J. Agron. 18 (3), 235–265.
Khaleel, R., Yeh, T.C.J., Lu, Z., 2002. Upscaled flow and transport properties for heterogeneous unsaturated media. Water Resour. Res. 38 (5), 1053–1065.
Kendy, E., Gérard-Marchant, P., Walter, M.T., Zhang, Y.Q., Liu, C.M., Steenhuis, T.S., 2003. A soil-water-balance approach to quantify groundwater recharge from irrigated cropland in the North China Plain. Hydrol. Process. 17 (10), 2011–2031.
Liu, Z., Zha, Y.Y., Yang, W.Y., Kuo, Y.M., Yang, J.Z., 2016. Large-scale modeling of unsaturated flow by a stochastic perturbation approach. Vadose Zone J. 15 (3).
Luo, Y.F., Jiang, Y.L., Peng, S.Z., Khan, S., Cai, X.L., Wang, W.G., Jiao, X.Y., 2012. Urban weather data to estimate reference evapotranspiration for rural irrigation management. J. Irrig. Drain. Eng. 138 (9), 837–842.
Matthews, C.J., Cook, F.J., Knight, J.H., Braddock, R.D., 2005a. Handling the water content discontinuity at the interface between layered soils within a numerical scheme. Aust. J. Soil Res. 43, 945–955.
Matthews, C.J., Knight, J.H., Cook, F.J., Braddock, R.D., 2005b. Using analytical solutions for homogeneous soils to assess numerical solutions for layered soils. Available at https://research-repository.griffith.edu.au/bitstream/handle/10072/2735/29373_1.pdf?sequence=1.
Merritt, W.S., Letcher, R.A., Jakeman, A.J., 2003. A review of erosion and sediment transport models. Environ. Modell. Softw. 18 (8), 761–799.
Pan, F., Nieswiadomy, M., Qian, S., 2015. Application of soil moisture diagnostic equation for estimating root-zone soil moisture in arid and semi-arid regions. J. Hydrol. 524, 296–310.
Raes, D., 2002. BUDGET: a soil water and salt balance model. Reference manual, version 5, http://iupware.be/?page_id=820.
Ranatunga, K., Nation, E.R., Barratt, D.G., 2008. Review of soil water models and their applications in Australia. Environ. Modell. Softw. 23 (9), 1182–1206.
Ratliff, L.F., Ritchie, J.T., Cassel, D.K., 1983. Field-measured limits of soil water availability as related to laboratory-measured properties. Soil Sci. Soc. Am. J. 47 (4), 770–775.
Rengasamy, P., 2006. World salinization with emphasis on Australia. J. Exp. Bot. 57 (5), 1017–1023.
Richardson, L.F., 1922. Weather Prediction by Numerical Process. Cambridge University Press.
Riha, S.J., Rossiter, D.G., Simoens, P., 1994. GAPS: General-purpose atmosphere-plant-soil simulator Version 3.0 User's Manual. SCAS Teaching Series Cornell University, Department of Soil, Crop & Atmospheric Sciences, Ithaca, New York.
Schoups, G., Hopmans, J.W., Tanji, K.K., 2006. Evaluation of model complexity and space-time resolution on the prediction of long-term soil salinity dynamics, western San Joaquin Valley, California. Hydrol. Process. 20 (13), 2647–2668.
Sheikh, V., Visser, S., Stroosnijder, L., 2009. A simple model to predict soil moisture: bridging event and continuous hydrological (BEACH) modelling. Environ. Modell. Softw. 24 (4), 542–556.
Shen, C., Phanikumar, M.S., 2010. A process-based, distributed hydrologic model based on a large-scale method for surface-subsurface coupling. Adv. Water Resour. 33 (2), 1524–1541.
Šimunek, J., Šejna, M., Saito, H., Sakai, M., van Genuchten, M.Th., 2008. The HYDRUS-1D Software Package for Simulating the Movement of Water, Heat, and Multiple Solutes in Variably Saturated Media, Version 4.0, HYDRUS Software Series 3, Department of Environmental Sciences, University of California Riverside, Riverside, California.
Šimůnek, J., Šejna, M., van Genuchten, M.Th., 2012. The UNSATCHEM Module for HYDRUS (2D/3D) Simulating Two-Dimensional Movement of and Reactions Between Major Ions in Soils, Version 1.0, PC Progress, Prague, Czech Republic.
Skagges, R.W., Monke, E.J., Huggins, L.F., 1970. An approximate method for determining the hydraulic conductivity function of an unsaturated soil. Techn. Rep. No. 11, Water Resour. Res. Center, Purdue University, Lafayette.
Sluiter, R., 1998. Desertification and Grazing On south Crete, A model approach. Department of Physical Geography, Faculty of Geographical Sciences, University of Utrecht, Utrecht.
Sun, H.W., Zhu, Y., Yang, J.Z., Wang, X.G., 2015. Global sensitivity analysis for an integrated model for simulation of nitrogen dynamics under the irrigation with treated wastewater. Environ. Sci. Pollut. Res. 22 (21), 16664–16675.
Vaccaro, J., 2007. A deep percolation model for estimating ground-water recharge: Documentation of modules for the modular modeling system of the U.S. Geological Survey, https://pubs.er.usgs.gov/publication/sir20065318.
Valipour, M., 2014. Drainage, waterlogging, and salinity. Arch. Agron. Soil Sci. 60 (12), 1625–1640.
Valipour, M., 2015. Comparative evaluation of radiation-based methods for estimation of potential evapotranspiration. J. Hydrol. Eng. 20 (5), 04014068.
Van Genuchten, M.T., 1980. A closed-form equation for predicting the hydraulic conductivity of unsaturated soils. Soil Sci. Soc. Am. J. 44 (5), 892–898.
Verburg, K., 1995. Methodology in soil water and solute balance modelling: an evaluation of APSIM-SoilWat and SWIMv2 models. Report of APSRU. CSIRO Division of Soils Workshop, Brisbane, Qld.
Vereecken, H., Weynants, M., Javaux, M., Pachepshy, Y., Schaap, M.G., van Genuchten, M.T., 2010. Using pedotransfer functions to estimate the van Genuchten-Mualem soil hydraulic properties: a review. Vadose Zone J. 9 (4), 795–820.
Vereecken, H., Schnepf, A., Hopmans, J.W., Javaux, M., Or, D., Roose, T., Vanderborght, J., Young, M.H., Amelung, W., Aitkenhead, M., Allison, S.D., Assouline, S., Baveye, P., Berli, M., Brüggemann, N., Finke, P., Flury, M., Gaiser, T., Govers, G., Ghezzehei, T., Hallett, P., Hendricks Franssen, H.J., Heppell, J., Horn, R., Huisman, J.A., Jacques, D., Jonard, F., Kollet, S., Lafolie, F., Lamorski, K., Leitner, D., McBratney, A.B., Minasny, B., Montzka, C., Nowak, W., Pachepsky, Y., Padarian, J., Romano, N., Roth, K., Rothfuss, Y., Rowe, E.C., Schwen, A., Šimunek, J., Tiktak, A., Van Dam, J., van der Zee, S.E.A.T.M., Vogel, H.J., Vrugt, J.A., Wöhling, T., Young, I.M., 2016. Modeling soil processes: review, key challenges, and new perspectives. Vadose Zone J. 15 (5). https://doi.org/10.2136/vzj2015.09.0131.
Wang, L., 2007. Experiment and Simulation of Transformation and Transport of Nitrogen and Phophorus in Saturated-unsaturated Soils. Wuhan University, Wuhan.
Wang, X., Williams, J.R., Gassman, P.W., Baffaut, C., Izaurralde, R.C., Jeong, J., Kiniry, J. R., 2012. EPIC and APEX: model use, calibration, and validation. Trans. ASABE 55 (4), 1447–1462.
Wesseling, J.G., 2009. Soil Physical Data and Modeling Soil Moisture Flow. Wageningen University, Wageningen.
Westenbroek, S.M., Kelson, V., Dripps, W., Hunt, R., Bradbury, K., 2010. SWB-A modified Thornthwaite-Mather Soil-Water-Balance code for estimating groundwater recharge. US Geological Survey, https://pubs.er.usgs.gov/publication/tm6A31.
Xu, T.F., Spycher, N., Sonnenthal, E., Zhang, G.X., Zheng, L.G., Pruess, K., 2012. TOUGHREACT user's guide: A simulation program for non-isothermal multiphase reactive transport in variably saturated geologic media, version 2.0. Earth Sciences Division, Lawrence Berkeley National Laboratory, Berkeley.
Yang, D., Zhang, T., Zhang, K., Greenwood, D.J., Hammond, J.P., White, P.J., 2009. An easily implemented agro-hydrological procedure with dynamic root simulation for water transfer in the crop-soil system: validation and application. J. Hydrol. 370 (1), 177–190.
Yang, J.Z., Zhu, Y., Zha, Y.Y., Cai, S.Y., 2016. Mathematical Model and Numerical Method of Groundwater and Soil Water Movement. Science Press, Beijing.
Zha, Y.Y., 2014. Research on Cost-effective Algorithm for Unsaturated-saturated Flow and its Application. Wuhan University, Wuhan.
Zha, Y.Y., Yang, J.Z., Shi, L.S., Song, X.H., 2013. Simulating one-dimensional unsaturated flow in heterogeneous soils with water content-based Richards equation. Vadose Zone J. 12, 1–12.
Zha, Y.Y., Yeh, T.C.J., Illman, W.A., Onoe, H., Mok, C.M.W., Wen, J.C., Huang, S.Y., Wang, W.K., 2017. Incorporating geologic information into hydraulic tomograhpy: a general framework based on geostatistical approach. Water Resour. Res. 53 (4), 2850–2876.
Zhu, Y., Yang, J.Z., Wang, L.Y., 2009. Experimental, numerical and sensitive analysis of nitrogen dynamics in soils irrigated with treated sewage. Sci. China Ser. E Technol. Sci. 52 (11), 3279–3286.
Zhu, Y., Yang, J.Z., Ye, M., Sun, H.W., Shi, L.S., 2017. Development and application of a fully integrated model for unsaturated-saturated nitrogen reactive transport. Agric. Water Manage. 180, 35–49.